Topological doping of a three-dimensional Peierls system: Predicted structure of doped BaBiO$_3$

Ilka B. Bischofs,[1,*] Philip B. Allen,[1] Vladimir N. Kostur,[1,†] and Rahul Bhargava[1,2,‡]

[1]*Department of Physics and Astronomy, State University of New York, Stony Brook, New York 11794-3800*
[2]*The Wheatley School, 11 Bacon Road, Old Westbury, New York 11568*

At hole concentrations below $x = 0.4$, Ba$_{1-x}$K$_x$BiO$_3$ is nonmetallic. At $x = 0$, pure BaBiO$_3$ is a Peierls insulator. Very dilute holes create bipolaronic point defects in the Peierls order parameter. Here we find that the Rice-Sneddon version of Peierls theory predicts that more concentrated holes should form stacking faults (two-dimensional topological defects, called "slices") in the Peierls order parameter. However, the long-range Coulomb interaction, left out of the Rice-Sneddon model, destabilizes slices in favor of point bipolarons at low concentrations, leaving a window near 30% doping where the sliced state is marginally stable.

I. INTRODUCTION

When a one-dimensional (1D) crystal is driven incommensurate, for example, by doping to alter the Fermi wave vector, it is well known that the modulation of the commensurate crystalline order tends not to be uniform but to accumulate at kinks in the crystalline order parameter.[1] A prototype for this is the Su-Schrieffer-Heeger model[2] for polyacetylene [(CH)$_x$]. In a simple chemical view, the carbon chain has alternating single and double bonds. Crystallography confirms this lattice dimerization. The scalar order parameter (amplitude of the staggered charge disproportionation) has two possible values $\pm \rho$. Zero-dimensional domain walls (topological defects) separate regions of the 1D chain with positive and negative order parameters. Su *et al.* showed that when carriers are doped into polyacetylene, they create new domain-wall defects and localize into midgap electronic soliton states on these defects. Analogous effects in two dimensions[3] occur in layered materials near a Mott insulator phase, such as cuprates, nickelates, and layered manganites. The one-dimensional domain wall in the 2D system is generally called a "stripe." The 3D analog, which occurs in some cubic manganites,[4] is a planar domain wall,[5] sometimes called a "sheet" or "lamella." We prefer the term "slice," which like the word "stripe" can be used as a verb or noun. Here we discuss a 3D model system in which bonding and strain energies favor slices, but long-range Coulomb interactions prefer point defects. We analyze the system numerically and show that at doping levels near 30%, Ba$_{1-x}$K$_x$BiO$_3$ is near the crossover where slices may become more favorable than point defects for lowering the energy of the doped-in holes.

Charge-density-wave (CDW) and Peierls systems have scalar order parameters $\rho_Q = N^{-1} \Sigma_\ell \rho_\ell \exp(i\vec{Q} \cdot \vec{\ell})$. BaBiO$_3$ is a simple 3D example. With nominal valence Bi^{4+}, the Bi 6s band is half-filled. The material is nonmetallic, with a 2-eV optical gap.[6] Crystallography[7] shows a doubled unit cell; ρ_ℓ alternates with wave vector $Q = (\pi, \pi, \pi)$. The simple cubic sublattice of nominal Bi^{4+} ions self-organizes into a bipartite (rocksalt-type) charge-ordered array of nominal Bi^{3+} ($\rho = 4 - \rho_Q$, called "A" sites) and nominal Bi^{5+} ($\rho = 4 + \rho_Q$, called "B" sites) ions. The actual value of the order parameter ρ_Q has magnitude $\leqslant 1$ and takes two degenerate values

$\pm |\rho_Q|$. A simple way to think of this is as a 3D version of a Peierls instability. In a bipartite lattice with only nearest-neighbor hopping there is accidental Fermi surface nesting, $\epsilon(\vec{k}) = -\epsilon[\vec{k} + (\pi, \pi, \pi)]$, and both are zero at the Fermi energy. This guarantees that the crystal can reduce its electronic band energy via the electron-phonon interaction by dimerizing. A Hamiltonian which contains this effect was introduced by Rice and Sneddon.[8,9]

Regions of charge-ordered BaBiO$_3$ with $\rho_Q > 0$ are separated from regions with $\rho_Q < 0$ by stacking faults. The simplest stacking fault lies in a (111) plane. In perfectly ordered BaBiO$_3$, (111) planes are alternating A and B type [Fig. 1(a)]. A stacking fault with no nuclear disorder has either two adjacent A layers (local charge excess -1 per site on the plane or electron doped) or two adjacent B layers (local charge excess 1 or hole doped) as in Fig. 1(b).

Here we point out that the Rice-Sneddon Hamiltonian, given below, predicts that holes or electrons, when introduced, will self-organize into slices. However, the long-range Coulomb interaction, neglected in the Rice-Sneddon model, will destabilize slices except possibly at the most favorable doping level. For light doping, the preferred structure for holes is to self-organize into point defects, small bipolarons, as previously discussed.[10–13]

II. RICE-SNEDDON MODEL

The Rice-Sneddon model[8] is simple, well studied,[9,10,14,15] and quite successful.[12,13] In the perovskite crystal structure of
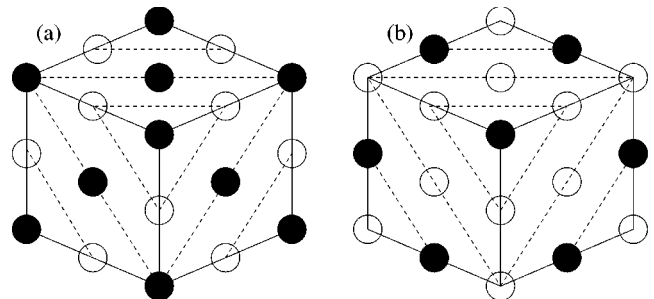

FIG. 1. Fragment of BaBiO$_3$, showing Bi atoms only. Solid circles are Bi^{3+} (A) ions, and open circles are Bi^{5+} (B) ions. In (a) the normal ABABAB . . . sequence of (111) layers is shown; in (b), a hole-type stacking fault ABBABA . . . , or slice, is shown.

$BaBiO_3$, each Bi atom is surrounded by six oxygens and each oxygen is shared by two Bi atoms. At high temperatures (of order 1000 K) the crystal is nearly cubic perovskite, but at lower T there are rotations and distortions of the BiO_6 octahedra, which enlarge the unit cell. We believe that the most important effect is the "breathing" displacements $u_0 \approx \pm 0.12$ Å (Refs. 7, 17, and 18) of oxygens away from or toward alternate Bi atoms. These provide a natural electron-phonon mechanism to enhance the Bi $6s$ charge density on A sites where oxygens breath outward and reduce the Bi $6s$ charge density on B sites where the oxygens breathe in. A microscopic Hamiltonian containing the minimal necessary electron-phonon interaction was given by Rice and Sneddon,[8]

$$\mathcal{H} = -t \sum_{\langle \ell, \ell' \rangle} c_\ell^\dagger c_{\ell'} - g \sum_\ell e(\vec{\ell}) c_\ell^\dagger c_\ell + \frac{1}{2} K \sum_{\ell, \alpha} u \left(\vec{\ell} + \frac{\hat{\alpha}}{2} \right)^2. \quad (1)$$

The first term is the nearest-neighbor hopping of Bi $6s$ electrons with hopping integral $t \approx 0.35$ eV. The index of summation ℓ implicitly includes a spin as well as site quantum number. The filling is $1-x$ electrons per site. The variable $u(\vec{\ell} + \hat{\alpha}/2)$ (with $\alpha = x, y, z$) is the displacement along a Bi-O-Bi bond in the $\hat{\alpha}$ direction of the oxygen located at position $(\vec{\ell} + \hat{\alpha}/2)a$. The variable $e(\ell)$ is the local dilation or "breathing" amplitude of the six oxygens which surround the Bi ion at site ℓ,

$$e(\ell) = [u(\vec{\ell} + \hat{x}/2) - u(\vec{\ell} - \hat{x}/2)] + [x \to y] + [x \to z]. \quad (2)$$

The Einstein restoring force $K \approx 19$ eV/Å^2 is fitted to the measured 70 meV frequency of the Raman-active Peierls breathing mode.[19]

At half-filling, this model opens a Peierls gap at the Fermi level; the electron-phonon interaction parameter $g \approx 1.39$ eV/Å is fitted to the measured[6] ≈ 2 eV gap. This is an ordinary size electron-phonon coupling. The change in Coulomb field of a charge $-2e$ oxygen ion gives $g \approx 1.2$ eV/Å. The resulting dimensionless coupling constant $\Gamma \equiv g^2/Kt$ is ≈ 0.30, intermediate between the weak ($\Gamma < 0.2$) and strong ($\Gamma > 0.4$) coupling regimes. In this middle regime, neither hopping nor electron-phonon energy dominates.[12] The ground state of undoped $BaBiO_3$ is as close to a bipolaronic crystal (large Γ, $|\rho_Q| \approx 1$) as to the conventional Peierls CDW (small Γ). We calculated[12] the order parameter ρ_Q at $\Gamma = 0.3$ to be 0.82. The corresponding oxygen displacement $u_0 = 2g\rho_Q/K = 0.12$ Å agrees with diffraction and extended x-ray absorption fine structure (EXAFS) measurements,[7,17,18] showing that the model is internally consistent.

We previously found that excitations across the Peierls gap form self-trapped excitons.[13] We also reported that holes inserted into $BaBiO_3$ self-trap and form bipolarons[12] since the coupling strength exceeds $\Gamma_c = 0.17$. These are doubly charged point defects, corresponding to local depressions of the order parameter where the oxygen distortion $e(\vec{\ell}) \to 0$ for $t = 0$. For nonzero hopping t the bipolaron spreads out and
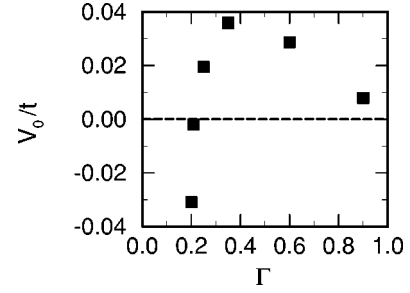

FIG. 2. Interaction potential V_0 for two bipolarons sitting on $(0,0,0)$ and $(a/2)(1,1,0)$. Large bipolarons attract whereas small bipolarons repel.

evolves continuously from a small bipolaron ($\Gamma \gg \Gamma_c$) to large CDW-like bipolaron as $\Gamma \to \Gamma_c$. The stability of bipolaron defects provides a simple explanation why dilutely doped $BaBiO_3$ remains insulating and diamagnetic.

The "disproportionation reaction" $2Bi^{4+} \to Bi^{3+} + Bi^{5+}$ has been much discussed in the literature on $BaBiO_3$. Using the definition $2U = E(Bi^{3+}) + E(Bi^{5+}) - 2E(Bi^{4+})$, one can say that the effective Hubbard U parameter is negative. Two factors may contribute to U: electron-phonon effects (expected to be attractive) and Coulomb repulsion ($U = U_{ep} + U_{el}$). If one wants to assign the mechanism for disproportionation completely to Coulomb interactions, then the Hubbard U calculated with all atoms held stationary in cubic perovskite positions (defined as U_{el}) should be negative. Vielsack and Weber[16] did careful calculations of U_{el}, finding no evidence for negative values, but instead a small positive value $U_{el} \approx 0.6 \pm 0.4$ eV. Therefore we shall temporarily ignore the on-site Coulomb repulsion U_{el}. Apparently the Bi^{4+} ion must reorganize its environment in order to stabilize the charge disproportionation.

III. HOLE DOPING

What happens at finite doping concentrations x? Assuming sufficient electron-phonon coupling to destroy the undistorted metal, there are two possibilities: (1) bipolarons and (2) slices.

(1) Numerical studies by Yu et al.,[10] and confirmed by us, show that randomly located point bipolarons are at least metastable. Depending on whether bipolarons attract or repel, the system could then either phase separate into undoped and doped regions or form spatially separated bipolarons. When bipolarons are small, the energy of an array of bipolarons is approximately described by a pairwise additive potential $V(\Gamma, r)$, containing the repulsive long-range Coulomb interaction V_{Coul} (neglected for the time being) and the interaction V_t, induced by hopping. V_t decays exponentially with the distance r between two bipolarons (like bipolaron wave functions.) Since bipolarons can only sit on former A sites, the nearest-neighbor interaction $V_0 = V_t(\Gamma, \sqrt{2}a)$, which is also the strongest interaction, is between bipolarons separated by $a(110)$. We computed V_0 numerically by optimizing the oxygen positions self-consistently for given bipolaron positions. Figure 2 shows that large CDW-like bipolarons attract each other, whereas small bipolarons repel, with V_t
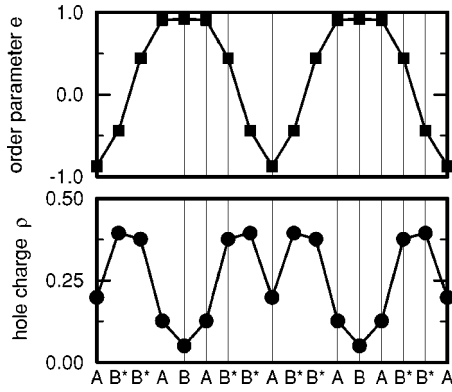
FIG. 3. Normalized breathing order parameter $e/6u_0$ (upper panel) and hole charge ρ_{hole} (lower panel) for a $x=1/4$ doped phase-slip structure $(AB^*B^*ABAB^*B^*)_N$ at $\Gamma=0.3$ (two periods shown). The order parameter changes sign across each phase slip B^*B^*. Holes are localized on phase-slip planes with slight spreading to neighboring A planes. The hole charge is computed relative to a reference system with the same structure, $(AB^*B^*ABAB^*B^*)_N$, but with A charges fixed at their undoped value $4+\rho_Q$, B charges fixed at $4-\rho_Q$, and B* charges fixed at $4-\rho_Q/2$ corresponding to zero doping, with the charge deficit ρ_Q spread equally on the two adjacent B* layers. The charge fluctuation ρ_Q has the value 0.82 at $\Gamma=0.3$.

$\rightarrow 0$ in the atomic limit $t\rightarrow 0$. Perturbation theory around $t=0$ gives a bipolaron repulsion. At the physically relevant value $\Gamma=0.3$, bipolarons repel according to Fig. 2, but multi-bipolaron interactions become important with decreasing Γ. Therefore, in the intermediate coupling regime we must rely on exact numerical diagonalization of Eq. (1).[10]

(2) In contrast to bipolaron defects where the order parameter never changes sign, holes could form topological defects. Phase slips are planar defects with sign changes of the charge order parameter ρ_Q and of the breathing order parameter $\hat{e}=(-1)^l e_l$. Consider a "BB" stacking fault in the 111 direction [Fig. 1(b)]. In the atomic ($t\rightarrow 0$) limit, each B site on a phase-slip plane has three displaced and three undisplaced oxygen neighbors, i.e., $e_l\approx\pm 3u_0$. Phase slips accumulate one hole for every two atoms on a (111) BB bilayer. The average hole charge on phase-slip B sites is thus $\rho_{hole}\approx+\frac{1}{2}$. The actual values of hole charge found for $\Gamma=0.3$ and $x=1/4$ are shown in Fig. 3.

Our aim is to find the ground-state hole arrangement, testing the stability of several bipolaronic (1) versus the phase-slip (2) solutions numerically. We did a series of calculations on $x=1/4$ doped systems. The bipolaron systems (1) were (a) maximal spacing between bipolarons, obtained when they occupy center and corner sites of a tetragonal 16-atom unit cell (*bct* structure); (b) a simple cubic (sc) arrangement of bipolarons sitting at the corner sites of a 8-atom cubic cell; (c) a disordered structure with random bipolaron positions; (d) phase-separated structures based on unit cells containing 8 or 16 (111) planes, where we replace one or two near-neighbor A planes with bipolaronic B planes, $[(AB)_3B_2]_N$ or $[(AB)_6B_4]_{N/2}$. We also looked at unit cells with 8 or 16 111 planes containing phase slips (2) $[AB(ABB)_2]_N$ and $[(AB)_2(ABB)_4]_{N/2}$. Finally, we looked at the undistorted
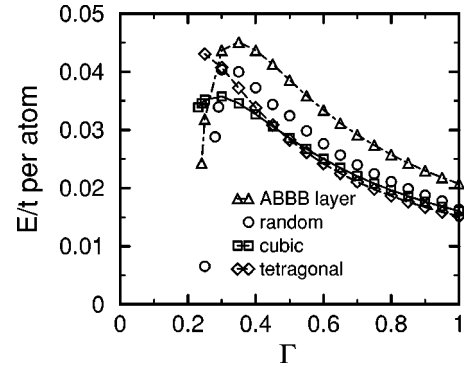

FIG. 4. Energy difference E/t of bipolaron structures (1a)–(1d) relative to the most favorable phase-slip structure (2) for $x=1/4$ doping.

metal $[C]_N$ where each atom C has a nominal $Bi^{4.25+}$ valence.

Phase separation was strongly disfavored, while separated bipolarons and phase slips were all metastable. The phase slips weakly repelled, preferring the 8-plane solution to the 16-plane solution. The order parameter and hole charge density of this 8-plane solution are shown in Fig. 3. The stability is determined computing the total energy $E_{tot}(\{u_{\vec{l}}\})$ given by Eq. (1), which is a function of the oxygen positions $u_{\vec{l}}$. We start by guessing oxygen positions to get close to a local minimum in the energy landscape, then vary the oxygen positions using a gradient minimization routine to find a self-consistent minimum. For smaller periodic structure, we used k-space sampling in the corresponding Brillouin zones (8000 $\vec{k}$ points). For each $\vec{k}$, $\mathcal{H}$ is diagonalized exactly. States are filled with two electrons up to the desired doping. For the random bipolaron structure we used large asymmetric clusters (≈ 400 atoms) with periodic boundary conditions and $k=0$ only. Initial oxygen positions had Peierls order with small random deviations. Our calculations on random configurations generally reproduce the earlier calculations of Yu *et al.*[10]

Energies of various states at doping $x=1/4$ are shown in Fig. 4. In the atomic limit $t=0$ all bipolaron and phase-slip structures are degenerate. All that is required is that no A site should have an A first neighbor. Below a critical coupling strength $\Gamma_c(x)$ (≈ 0.2 for doping $x=1/4$), distorted structures become unstable with respect to the undistorted metallic structure. Above $\Gamma_c(x)$, we find numerically that at $x=1/4$ holes strongly prefer to order in phase slips (2). Bipolaronic structures (1) are quite similar to each other in energy and behave as expected from the bipolaron-pair interaction. In the intermediate coupling range there occurs a crossover from the tetragonal to the layered BBB structure as a stable bipolaron configuration, corresponding to a change in the overall bipolaron interaction from weakly repulsive to weakly attractive. For 1/4-doped $BaBiO_3$, the energy gain for the phase-slip solution compared to the bipolarons is about 50–65 meV per hole.

Thus, contrary to previous studies of doping of this model,[9,10] we find that the stable doping state is not bipolarons but phase slips. Does this model correspond suffi-

ciently to reality for BaBiO$_3$? Iwano and Nasu[14] use a more complicated hopping and electron-phonon interaction, but we believe that such corrections are not the relevant ones. There are also (i) small structural distortions (rotations of oxygen octahedra) beyond the breathing-mode distortions considered here and (ii) nonadiabatic effects (such as zero-point motion) associated with the fact that the oxygen mass is not infinitely large compared with the electron mass. We believe that both of these also have little relevance. It is harder to dismiss two other effects: (iii) the disorder caused by the dopant atoms and (iv) the long-range Coulomb interaction, both omitted so far. Of these, the last is clearly important, as we now show, and tends to destabilize phase-slips relative to distributed bipolarons.

IV. LONG-RANGE COULOMB EFFECT

At low doping, there is a large Coulomb cost in putting charges onto stacking faults instead of widely distributed point charges. We modeled this as follows. The Madelung energy was computed by the Ewald method for $(Ba^{2+})_2(Bi^{3+}Bi^{5+})(O^{2-})_6$. The calculation was redone for many large unit cells, with holes added on selected Bi ions $(Bi^{3+} \rightarrow Bi^{5+})$ and compensating negative charges distributed uniformly throughout space. This is one way to mimic potassium doping of BaBiO$_3$. First consider the sliced state. By numerical calculation for uniformly distributed phase slips at many values of x between 1/39 and 1/3, we found a good fit to the formula $E_S = (-25.1 + \pi/9x)(e^2/2a\epsilon_\infty)$. The static electronic screening $\epsilon_\infty \approx 5$ was measured by Tajima *et al.*[20] E_S is the difference of energy per hole between the sliced solution and the undoped Peierls insulator. The term $\pi/9x$ is the analytic result for idealized uniform sheets of charge of vanishing thickness, arranged periodically in a compensating charge background. The term -25.1 corrects for the discreteness of the charges, the absence of the self-interaction, and includes the Coulomb energy of the holes with the background BaBiO$_3$ lattice.

We also need the energy difference per hole, E_B, of optimally spaced bipolarons relative to the undoped Peierls insulator. For doping $x = 1/n^3$ the bipolarons can be placed on a sublattice of face-centered-cubic (fcc) form, with maximum spacing. Numerical results for $n = 2$, 3, and 4 fitted well to the formula $E_B = (-21.2 - 4.585x^{1/3})(e^2/2a\epsilon_\infty)$. The term $-4.585x^{1/3}$ is the Madelung energy of an fcc lattice of charges $2e$ in a uniform compensating background, and the constant -21.2 accounts for the energy of the holes in the background BaBiO$_3$ lattice. The difference $E_S - E_B$ is the Coulomb penalty per hole for forming slices or phase slips. It is plotted in Fig. 5, becoming large at low x with a shallow minimum near $x = 0.3$.

A more accurate estimate of the Coulomb penalty is shown as an **x** in Fig. 5 and was obtained by doing Ewald sums using the actual Bi site charges ($\rho_i = 5 - n_i$ where $n_i = 2\langle\psi_i^\dagger\psi_i\rangle$ is the local occupancy of the Bi s states) and the actual $(AB*B*ABAB*B*)_N$ slice structure and body-centered-tetragonal (bct) bipolaron structure. It is seen in the figure that at 1/4 doping, the Coulomb penalty is twice as high as the Peierls benefit in forming slices. These calcula-
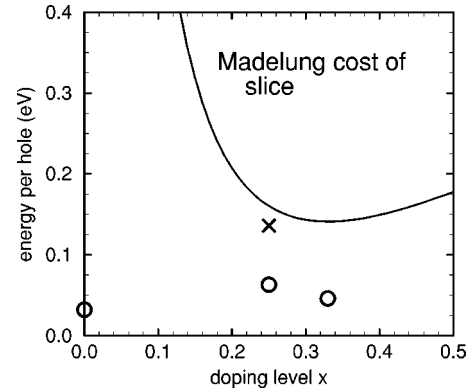

FIG. 5. The curve is an analytic approximation to the Madelung or Coulomb repulsion of a periodic array of (111) phase slips (slices) compared with optimally spaced separated bipolarons at the same average density, where doped-in holes are modeled as point charges (charge$= e$) with screening ϵ_∞ set to 5. The open circles give the numerically computed Peierls short-range stabilization energy (from hopping and electron-phonon energy) of sliced solutions relative to separated bipolarons. The symbol **x** is the exact numerical Madelung energy difference at 1/4 doping between the sliced solution and the bct bipolaron solution with the numerically computed layer charges ρ_i.

tions did not account for the actual random positions of the compensating negative charges where Ba^{2+} ions are replaced by K$^+$ ions. Instead, the compensating charge was distributed uniformly. The calculations were repeated for a model where the compensating negative charges were equally shared by each Ba atom $(Ba^{2+} \rightarrow Ba^{(2-x)+})$. This only changed the constant terms in E_S and E_B, but did not affect the difference $E_S - E_B$ plotted here.

The Madelung sums discussed above are not the complete Coulomb effect. The missing on-site repulsion has the opposite effect, preferring sliced solutions to distributed bipolarons. If we add back the local term

$$\mathcal{H}_U = U_{el}\sum_i (\rho_i - 4)^2 \qquad (3)$$

and treat it as a first-order perturbation, the sliced solution at 1/4 doping has a lower on-site energy by $0.121U_{el}$ per hole than the bct bipolaron solution. Using the value $U_{el} \approx 0.6 \pm 0.4$ eV from Vielsack and Weber,[16] the on-site correction 0.07 ± 0.05 eV is potentially sufficient to restabilize the sliced solution. Thus we can say that the best place to look for sliced structures in BaBiO$_3$ is in the range near $1/4-1/3$ doping, but we cannot predict whether the sliced solution will be destroyed by disorder or Coulomb effects.

V. DIFFRACTION

Doping $x = 1/3$ is the highest at which a simple sliced solution $[(ABB)_N]$ is possible. For higher doping, either the A planes acquire polaron defects or the sliced solution is destroyed locally and purely bipolaronic regions invade.

Sliced structures will show up weakly as satellite reflections from the new [111] planar electron charge modulations.

In undoped $BaBiO_3$, the dimerized (Peierls) structure creates weak satellite Bragg peaks at wave vectors $\vec{G} \pm \Delta\vec{G}$, where $\vec{G}$ is a reciprocal lattice vector of the parent (simple cubic in our model) lattice and $\Delta\vec{G}$ is $(2\pi/a)(1/2, 1/2, 1/2)$. The satellites are in the centers of the cubic lattice of parent Bragg peaks. For the $(ABB)_N$ sliced structure, in a hypothetical single-domain sample, the $\Delta\vec{G} = (2\pi/a)(1/2, 1/2, 1/2)$ satellites are replaced by $\Delta\vec{G} = (2\pi/a)(1/3, 1/3, 1/3)$ satellites. In general, twinning of the four different [111]-plane sliced domains is expected, and there will be eight weak satellites in each unit cell of the parent reciprocal lattice.

In the $x = 1/4$ doped $[AB(ABB)_2]_N$ structure, the satellites are at $\Delta\vec{G} = (2\pi/a)(n/8, n/8, n/8)$ where $n = 1,2,3,4$, plus the three other equivalent diagonals corresponding to domains with other orientations. Ordering of the sliced superstructures will probably not be perfect, so the expectation is that the satellites may appear as streaks in the [111] and equivalent directions.

It is worth mentioning that there have been reports[21] (subsequently attributed to electron beam heating effects[22]) of superlattice diffraction spots in doped $BaBiO_3$, not apparently identical to the superstructures predicted here. A further search in the doping region $0.2 < x < 0.35$ would be interesting.

*Present address: Max-Planck-Institut für Kolloid- und Grenzflächenforschung, D-14424 Potsdam, Germany.

†Present address: AIG Financial Products, Westport, CT 06880.

‡Present address: Princeton University, Princeton, NJ 08544.

[1] V. L. Pokrovsky and A.L. Talapov, *Theory of Incommensurate Crystals* (Harwood Academic, New York, 1984).

[2] W.P. Su, J.R. Schrieffer, and A.J. Heeger, Phys. Rev. B **22**, 2099 (1980).

[3] J. Zaanen and O. Gunnarsson, Phys. Rev. B **40**, 7391 (1989).

[4] S. Mori, C.H. Chen, and S.-W. Cheong, Nature (London) **392**, 473 (2001).

[5] D.I. Khomskii and K.I. Kugel, Europhys. Lett. **55**, 208 (2001).

[6] R.P.S.M. Lobo and F. Gervais, Phys. Rev. B **52**, 13 294 (1995).

[7] D.E. Cox and A.W. Sleight, Solid State Commun. **19**, 969 (1976).

[8] T.M. Rice and L. Sneddon, Phys. Rev. Lett. **47**, 689 (1982); P. Prelovsek, T.M. Rice, and F.C. Zhang, J. Phys. C **20**, L229 (1987).

[9] E. Jurczek and T.M. Rice, Europhys. Lett. **1**, 225 (1986); E. Jurczek, Phys. Rev. B **35**, 6997 (1987).

[10] J. Yu, X.-Y. Chen, and W.P. Su, Phys. Rev. B **41**, 344 (1990).

[11] P.B. Allen and V. Kostur, Z. Phys. B: Condens. Matter **104**, 605 (1997).

[12] I.B. Bischofs, V.N. Kostur, and P.B. Allen, Phys. Rev. B **65**, 115112 (2002).

[13] P.B. Allen and I.B. Bischofs, Phys. Rev. B **65**, 115113 (2002).

[14] K. Iwano and K. Nasu, Phys. Rev. B **57**, 6957 (1998).

[15] P. Piekarz and J. Konior, Physica C **329**, 121 (2000).

[16] G. Vielsack and W. Weber, Phys. Rev. B **54**, 6614 (1996).

[17] C. Chaillout and A. Santoro, Solid State Commun. **65**, 363 (1988).

[18] J.B. Boyce, F.G. Bridges, T. Claeson, T.H. Geballe, G.G. Li, and A.W. Sleight, Phys. Rev. B **44**, 6961 (1991).

[19] S. Tajima, M. Yoshida, N. Koshizuka, H. Sato, and S. Uchida, Phys. Rev. B **46**, 1232 (1992).

[20] S. Tajima, S. Uchida, A. Masaki, H. Takagi, K. Kitazawa, S. Tanaka, and A. Katsui, Phys. Rev. B **32**, 6302 (1985).

[21] S. Pei, N.J. Zaluzec, J.D. Jorgensen, B. Dabrowski, D.G. Hinks, A.W. Mitchell, and D.R. Richards, Phys. Rev. B **39**, 811 (1989).

[22] M. Verwerft, G. Van Tendeloo, D.G. Hinks, B. Dabrowski, D.R. Richards, A.W. Mitchell, D.T. Marx, S. Pei, and J.D. Jorgensen, Phys. Rev. B **44**, 9547 (1991); P. Wochner, Q.J. Wang, S.C. Moss, S.K. Sinha, G. Grübel, H. Chou, L.E. Berman, J.D. Axe, C.-K. Loong, J.Z. Liu, W.D. Mosley, P. Klavins, and R.N. Shelton, *ibid.* **47**, 9120 (1993); C.H. Du, P.D. Hatton, H.Y. Tang, and M.K. Wu, J. Phys.: Condens. Matter **6**, L575 (1994).